Somatic loss of BRCA1 and p53 in mice induces mammary tumors with features of human *BRCA1*-mutated basal-like breast cancer

Xiaoling Liu*, Henne Holstege*, Hanneke van der Gulden*, Marcelle Treur-Mulder*†, John Zevenhoven‡, Arno Velds§, Ron M. Kerkhoven§, Martin H. van Vliet*¶, Lodewyk F. A. Wessels*¶, Johannes L. Peterse‖, Anton Berns‡, and Jos Jonkers*,**

Divisions of *Molecular Biology and ‡Molecular Genetics and Centre for Biomedical Genetics, §Central Microarray Facility, and ‖Department of Pathology, Netherlands Cancer Institute, Plesmanlaan 121, 1066 CX, Amsterdam, The Netherlands; and ¶Faculty of Electrical Engineering, Mathematics, and Computer Science, Delft University of Technology, Mekelweg 4, 2628 CD, Delft, The Netherlands

Edited by Inder M. Verma, The Salk Institute for Biological Studies, La Jolla, CA, and approved June 1, 2007 (received for review March 30, 2007)

Women carrying germ-line mutations in *BRCA1* are strongly predisposed to developing breast cancers with characteristic features also observed in sporadic basal-like breast cancers. They appear as high-grade tumors with high proliferation rates and pushing borders. On the molecular level, they are negative for hormone receptors and ERBB2, display frequent TP53 mutations, and express basal epithelial markers. To study the role of BRCA1 and P53 loss of function in breast cancer development, we generated conditional mouse models with tissue-specific mutation of *Brca1* and/or *p53* in basal epithelial cells. Somatic loss of both BRCA1 and p53 resulted in the rapid and efficient formation of highly proliferative, poorly differentiated, estrogen receptor-negative mammary carcinomas with pushing borders and increased expression of basal epithelial markers, reminiscent of human basal-like breast cancer. BRCA1- and p53-deficient mouse mammary tumors exhibit dramatic genomic instability, and their molecular signatures resemble those of human *BRCA1*-mutated breast cancers. Thus, these tumors display important hallmarks of hereditary breast cancers in *BRCA1*-mutation carriers.

mouse models | conditional knockout

Germ-line mutations in the human breast cancer susceptibility gene *BRCA1* are responsible for 40% to 50% of hereditary breast cancers and confer increased risk for development of ovarian, colon, and prostate cancers (1, 2). BRCA1 has been implicated in various cellular processes, including maintenance of genome integrity, DNA replication and repair, chromatin remodeling, and transcriptional regulation (3, 4). Although the exact mechanism of mammary tumor suppression by BRCA1 remains largely unknown, cells with dysfunctional BRCA1 show defects in survival and proliferation, increased radiosensitivity, chromosomal abnormalities, G_2/M checkpoint loss, and impaired homologous recombination repair (5).

BRCA1-mutated breast cancers that arise in women with germ-line mutations in *BRCA1* are high-grade, hormone receptor-negative breast carcinomas with frequent mutation of *TP53* (4, 6). They also possess a basal-like phenotype as defined by the expression of markers that are typical for basal/myoepithelial cells, such as the basal cytokeratins (CKs) CK5/6 and CK14 (7). Indeed, strong molecular similarities are observed between hereditary *BRCA1*-mutated breast cancers and sporadic basal-like breast carcinomas (8, 9). This phenotypic overlap has led to the hypothesis that sporadic basal-like cancers may have defects in BRCA1-related pathways, such as the amplification of *EMSY* and the methylation of *BRCA1* and *FANCF* (10).

Despite the fact that several mouse strains with conventional or conditional mutations in *Brca1* have been generated (11), no good mouse model for *BRCA1*-mutated basal-like breast cancer has been developed so far. Most conventional *Brca1* knockouts are embryonic-lethal when bred to homozygosity, yet heterozygous *Brca1* female mice are not tumor-prone (12–14). Hypomorphic $Brca1^{tr/tr}$ and $Brca1^{\Delta 11/\Delta 11}$;$p53^{+/-}$ mutant mice, as well as conditional MMTV*cre*;$Brca1^{Co/Co}$ and MMTV*cre*;$Brca1^{Co/Co}$;$p53^{+/-}$ mice develop mammary tumors with diverse histological patterns (15–17). Moreover, Cre-mediated recombination of the most widely used conditional *Brca1* allele ($Brca1^{Co}$) (18) generates a hypomorphic $Brca1^{\Delta 11}$ allele, which encodes BRCA1-Δ11, a naturally occurring splice variant of *Brca1* (19). Mouse mammary tumor models based on conditional *Brca1*-null alleles are therefore required to study the role of BRCA1 in breast cancer development.

Here we have generated conditional mouse mutants with somatic deletion of *Brca1* and *p53* in several epithelial tissues including mammary epithelium. Female mice of this strain showed a high incidence of mammary tumors that mimic many aspects of human *BRCA1*-mutated basal-like breast cancer.

Results

Somatic Inactivation of p53 Induces Mammary Tumor Formation. Because *BRCA1*-mutated breast tumors frequently contain mutations in *TP53* (20), we set out to create a mouse mammary tumor model based on simultaneous inactivation of BRCA1 and p53. Modeling mammary tumorigenesis in conventional *p53* knockout mice is complicated by the fact that these mice develop lymphomas and sarcomas, rather than epithelial tumors (21–23). Moreover, conventional tumor suppressor gene knockout mice do not mimic sporadic tumor development because the targeted mutations are present in all cells of the animal (24). We therefore generated a conditional mammary tumor model based tissue-specific inactivation of p53. To this end, we crossed conditional $p53^{F}$ mice with K14*cre* transgenic mice in which Cre recombinase expression is restricted to several epithelial tissues, including skin and mammary gland epithelium (25). The resulting K14*cre*;$p53^{F/F}$ female mice developed mammary tumors and skin tumors with a median latency (T_{50}) of 288 days (Fig. 1*A*).

Author contributions: X.L., A.B., and J.J. designed research; X.L., H.H., H.v.d.G., M.T.-M., J.Z., and J.J. performed research; X.L., H.H., H.v.d.G., M.T.-M., A.V., R.M.K., M.H.v.V., L.F.A.W., J.L.P., and J.J. analyzed data; and X.L. and J.J. wrote the paper.

The authors declare no conflict of interest.

This article is a PNAS Direct Submission.

Abbreviations: CGH, comparative genomic hybridization; CK, cytokeratin; CNA, copy number aberration; ER, estrogen receptor; GO, gene ontology; GSEA, gene set enrichment analysis; IDC-nos, invasive ductal carcinoma not otherwise specified; K–M, Kaplan–Meier; T_{50}, median latency.

Data deposition: Microarray expression data have been deposited in the ArrayExpress database, www.ebi.ac.uk/arrayexpress (accession no. E-NCMF-6).

†Deceased November 20, 2004.

**To whom correspondence should be addressed. E-mail: j.jonkers@nki.nl.

This article contains supporting information online at www.pnas.org/cgi/content/full/0702969104/DC1.

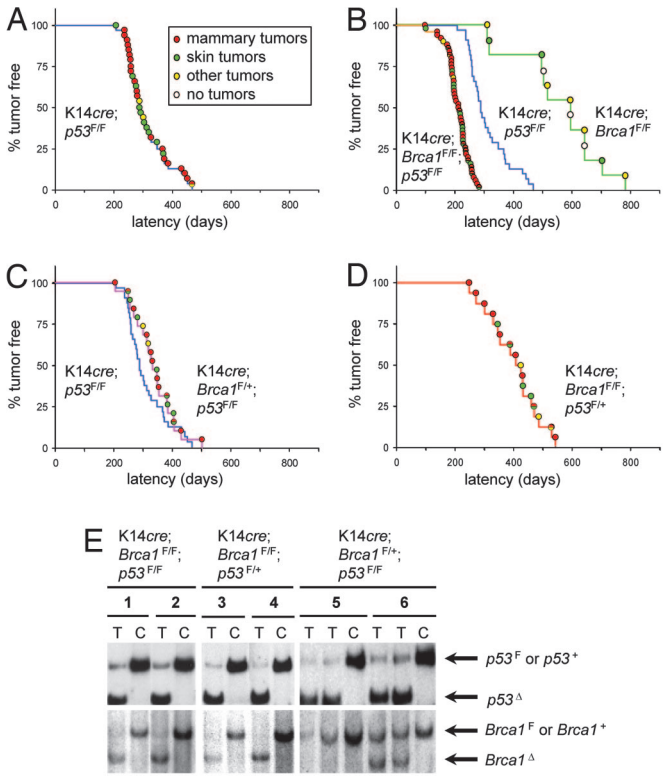

Fig. 1. Incidence and spectrum of tumors in K14*cre* female mice carrying conditional $Brca1^{F}$ and $p53^{F}$ alleles. (*A*) Kaplan–Meier (K–M) survival curve of K14*cre*;$p53^{F/F}$ female mice ($n = 32$) showing a median tumor-free survival age (T_{50}) of 288 days. (*B*) K–M curves of K14*cre*;$p53^{F/F}$ mice (blue curve) versus K14*cre*;$Brca1^{F/F}$ female mice (green curve; $n = 11$; $T_{50} = 595$ days; $P < 0.0001$) and K14*cre*;$Brca1^{F/F}$;$p53^{F/F}$ female mice (orange curve; $n = 50$; $T_{50} = 213$ days; $P < 0.0001$). (*C*) K–M curve of K14*cre*;$p53^{F/F}$ mice (blue curve) versus K14*cre*;$Brca1^{F/+}$;$p53^{F/F}$ female mice (pink curve; $n = 19$; $T_{50} = 332$ days; $P = 0.218$). (*D*) K–M curve of K14*cre*;$Brca1^{F/F}$;$p53^{F/+}$ female mice (red curve; $n = 16$; $T_{50} = 407$ days). Tumor types (mammary, skin, or other) are indicated for each female. Mice were killed when mammary tumors reached a diameter of ≈1 cm or skin tumors grew to a size of ≈0.7 cm. For mice with both skin and mammary tumors, the size of the latter was used as the criterion. (*E*) Southern blot analysis of tumor DNA to detect Cre-mediated deletion and spontaneous loss of *Brca1* (EcoRV + StuI digest, *Brca1* exon 14 probe) and *p53* (BglII digest, *p53* XbaI probe). Tumors (T) and control spleens (C) from the same animal are shown for representative female mice (1–6) of each genotype.

BRCA1 and p53 Loss Collaborate in Mouse Mammary Tumorigenesis. To study the role of BRCA1 in mammary tumorigenesis, we generated mice carrying conditional $Brca1^{F}$ alleles in which *Brca1* exons 5–13 are flanked by *loxP* sites [supporting information (SI) Fig. 7]. We crossed these animals to K14*cre* and K14*cre*;$p53^{F/F}$ mice to produce compound mutant animals with epithelium-specific loss of BRCA1 and/or p53. K14*cre*;$Brca1^{F/F}$ female mice showed normal ductal and alveolar development and were able to lactate and nurse their litters (data not shown). A cohort of 11 K14*cre*;$Brca1^{F/F}$ virgin mice was monitored for tumor formation; however, none of the animals developed mammary tumors during an 800-day period (Fig. 1*B*).

To study the potential synergistic effects of epithelial BRCA1 and p53 inactivation on mammary tumor formation, cohorts of K14*cre*;$Brca1^{F/F}$;$p53^{F/F}$, K14*cre*;$Brca1^{F/+}$;$p53^{F/F}$, and K14*cre*;$Brca1^{F/F}$;$p53^{F/+}$ female mice were generated and monitored for the development of neoplasms. Compared with K14*cre*;$p53^{F/F}$ animals, K14*cre*;$Brca1^{F/F}$;$p53^{F/F}$ mice developed mammary tumors with a significantly reduced T_{50} of 213 days (Fig. 1*B*; $P < 0.001$). Tumor onset and progression in these mice were relatively uniform, with most tumors arising between 140 and 280 days. Compared with K14*cre*;$Brca1^{F/F}$;$p53^{F/F}$ female mice, significantly longer median tumor-free survival periods ($P < 0.0001$) were observed for the K14*cre*;$Brca1^{F/+}$;$p53^{F/F}$ and K14*cre*;$Brca1^{F/F}$;$p53^{F/+}$ animals (T_{50} of 332 days and 407 days, respectively), demonstrating that both BRCA1 and p53 loss of function contribute to tumorigenesis in these mice (Fig. 1 *C* and *D*). K14*cre*;$Brca1^{F/+}$;$p53^{F/F}$ and K14*cre*;$p53^{F/F}$ animals developed tumors with comparable latency (Fig. 1*C*; $P = 0.218$), showing that BRCA1 is not haploinsufficient for suppression of mammary and skin tumorigenesis in mice. The fraction of female mice that developed mammary tumors was higher in the K14*cre*;$Brca1^{F/F}$;$p53^{F/F}$ cohort (40 of 50; 80%) than in the K14*cre*;$p53^{F/F}$ cohort (20 of 32; 63%), indicating that BRCA1 loss skews toward mammary tumorigenesis. Within each group, mammary and skin tumors developed with a comparable median latency, showing that BRCA1 and p53 loss of function also collaborate in skin tumorigenesis.

High Incidence of Loss of Heterozygosity at *p53*, but Not at *Brca1*, in Mammary Tumor Formation. Collaboration of BRCA1 and p53 inactivation in tumorigenesis was confirmed by Southern blot analysis of mammary tumors from K14*cre*;$Brca1^{F/F}$;$p53^{F/F}$, K14*cre*;$Brca1^{F/+}$;$p53^{F/F}$, and K14*cre*;$Brca1^{F/F}$;$p53^{F/+}$ mice. All tumors (32 of 32) from K14*cre*;$Brca1^{F/F}$;$p53^{F/F}$ mice had lost all four conditional $Brca1^{F}$ and $p53^{F}$ alleles (Fig. 1*E*, mice 1 and 2). Similarly, all tumors (11 of 11) from K14*cre*;$Brca1^{F/F}$;$p53^{F/+}$ animals showed Cre-mediated deletion of all conditional alleles as well as loss of the wild-type *p53* allele (Fig. 1*E*, mice 3 and 4). In contrast, in the K14*cre*;$Brca1^{F/+}$;$p53^{F/F}$ mice, all tumors (9 of 9) showed loss of both conditional Trp-53 alleles, but only 80% (7 of 9) of the tumors had lost the conditional *Brca1* alleles (Fig. 1*E*, mouse 6), and 20% (2 of 9) of the tumors showed retention of the conditional *Brca1* allele (Fig. 1*E*, mouse 5). None of these tumors showed loss of the wild-type *Brca1* allele. The stochastic loss of the conditional *Brca1* allele without concomitant loss of the wild-type allele suggests that BRCA1 has relatively weak tumor suppressor activity compared with p53 or that loss of heterozygosity at *Brca1* is more infrequent in mice than in humans.

Histopathologic Features of Mammary Tumors in K14*cre*;$p53^{F/F}$ and K14*cre*;$Brca1^{F/F}$;$p53^{F/F}$ Female Mice. As shown in Table 1 and SI Table 2, the mammary tumors that developed in K14*cre*;$p53^{F/F}$ female mice were either pure epithelial tumors (8 of 21; 38%), with glandular differentiation or a solid growth pattern without differentiation; or biphasic tumors either poorly differentiated with malignant epithelial and mesenchymal components (10 of 21; 48%) or differentiated with an organoid adenomyoepithelial pattern (3 of

Table 1. Mammary tumor spectrum and incidence in K*14cre;p53*$^{F/F}$ and K*14cre;Brca1*$^{F/F}$;*p53*$^{F/F}$ female mice

Tumor type	Human classification	Incidence (%)	
		K14*cre*;$p53^{F/F}$	K14*cre*;$Brca1^{F/F}$;$p53^{F/F}$
Carcinoma	Intermediate to high-grade IDC-nos	8/21 (38)	29/32 (91)
Biphasic carcinoma, poorly differentiated	Carcinosarcoma	10/21 (48)	1/32 (3)
Biphasic carcinoma, well differentiated	Adenomyoepithelioma	3/21 (14)	2/32 (6)

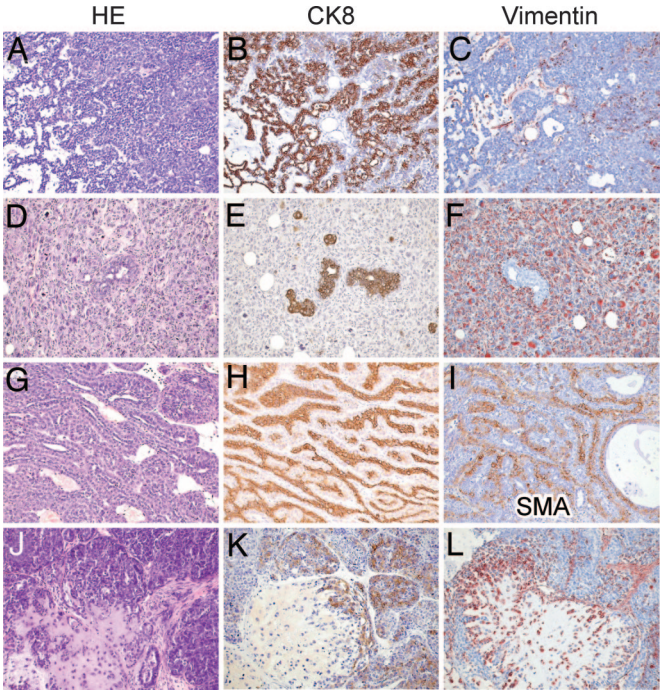

Fig. 2. Histopathological features of mammary tumors from K14*cre*;$p53^{F/F}$ and K14*cre*;$Brca1^{F/F}$;$p53^{F/F}$ female mice. Microphotographs of representative tumor sections stained with H&E (*A*, *D*, *G*, and *J*), or with antibodies against CK8 (*B*, *E*, *H*, and *K*), vimentin (*C*, *F*, and *L*), or smooth muscle actin (SMA) (*I*). (*A–C*) Solid carcinoma, resembling high-grade IDC-nos in humans. (*D–F*) Poorly differentiated biphasic carcinoma, resembling carcinosarcoma in humans. (*G–I*) Well differentiated biphasic carcinoma, resembling adenomyoepithelioma in humans. (*J–L*) Carcinoma with chondroid metaplasia.

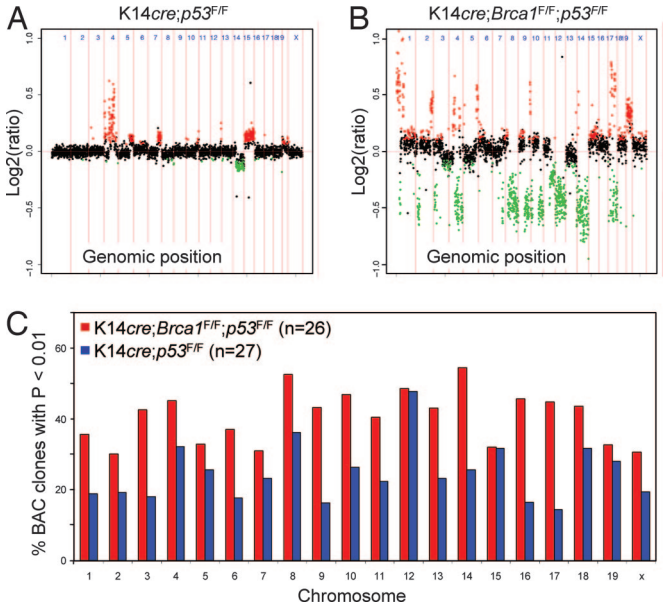

Fig. 3. Loss of BRCA1 induces genomic instability. (*A* and *B*) Array-CGH profiles of representative mammary tumors from K14*cre*;$p53^{F/F}$ and K14*cre*;$Brca1^{F/F}$;$p53^{F/F}$ mice, respectively. Log_2 hybridization ratios are plotted for 2,803 BAC clones, represented on the CGH microarray, at their genomic position. Red dots represent amplifications >0, and green dots represent deletions <0 (Rosetta error model; $P < 0.01$). (*C*) Comparison of array-CGH profiles of tumors from K14*cre*;$Brca1^{F/F}$;$p53^{F/F}$ ($n = 26$) and K14*cre*;$p53^{F/F}$ ($n = 27$) mice shows that BRCA1 loss results in a significant increase of CNAs. Depicted are mean percentages of BACs with a $P < 0.01$ per tumor group and per chromosome. Statistical significance of the observed differences in percentage of CNAs between both groups was calculated using a two-sided *t* test ($P = 0.00013$).

21; 14%). The pure epithelial tumors resembled human invasive ductal carcinoma not otherwise specified (IDC-nos) of intermediate to high grade; all showed expansive growth, high mitotic count, and moderate to high nuclear grade (Fig. 2 *A–C*). Necrosis was uncommon, and there was no or moderate lymphocytic infiltrate. The cells expressed CK8 and were ER-negative. The poorly differentiated biphasic tumors combined a high-grade CK8-positive epithelial component with a pleomorphic (malignant fibrous histiocytoma-like) CK8-negative and vimentin-positive mesenchymal component (Fig. 2 *D–F*). These tumors resembled human carcinosarcomas. The differentiated biphasic tumors resembled human adenomyoepitheliomas, showing complex branching glands lined by a double layer of CK8-expressing luminal epithelium and smooth muscle actin-positive myoepithelium (Fig. 2 *G–I*). Also these tumors had pushing borders, were estrogen receptor (ER)-negative and showed no or moderate lymphocytic infiltrate.

Compared with K14*cre*;$p53^{F/F}$ animals, a much larger fraction (29 of 32; 91%) of K14*cre*;$Brca1^{F/F}$;$p53^{F/F}$ female mice developed carcinomas that resembled high-grade IDC-nos in humans, with a solid growth pattern, a large CK8-positive and ER-negative cell type with high-grade nuclei, high mitotic count, and with pushing borders (Table 1 and SI Table 3). Few cases showed necrosis, and no or moderate lymphocytic infiltrate was observed. Some $Brca1^{\Delta/\Delta}$;$p53^{\Delta/\Delta}$ carcinomas (2 of 29; 7%) contained areas of chondroid metaplasia, with gradual transitions of solid nests of CK8-positive cells into dispersed CK8-negative, vimentin-positive (myoepithelial) cells surrounded by matrix (Fig. 2 *J–L*).

BRCA1 Loss Induces Genomic Instability. Genomic instability is an almost universal characteristic of solid tumors in humans (26), and both BRCA1 and p53 have been implicated in this phenomenon (27, 28). To assess the contribution of each tumor suppressor to genomic instability, we performed array-based comparative genomic hybridization (CGH) analysis on mammary tumors from K14*cre*;$p53^{F/F}$ and K14*cre*;$Brca1^{F/F}$;$p53^{F/F}$ female mice. Although somatic inactivation of p53 alone resulted in an appreciable level of genomic instability, as measured by the extent of DNA copy number aberrations (CNAs), combined inactivation of BRCA1 and p53 caused a significant increase in CNAs ($P = 0.00013$), indicating that BRCA1 loss of function is an important determinant for induction of genomic instability (Fig. 3).

BRCA1-Deficient Mouse Mammary Tumors Express Basal Epithelial Markers. To explore differences in gene expression between BRCA1-deficient and BRCA1-proficient mammary tumors, we determined the gene expression profiles of 32 $Brca1^{\Delta/\Delta}$;$p53^{\Delta/\Delta}$ tumors and 21 $p53^{\Delta/\Delta}$ tumors by using pooled RNA of 12 $p53^{\Delta/\Delta}$ tumors as a common reference. After combination of the normalized data from dye swap experiments using the Rosetta error model (29), 5,237 genes were selected that showed significant changes in expression across the 53 tumors. Next, a 2D unsupervised hierarchical clustering algorithm was used to group the 53 tumors on the basis of similarity in their gene expression profiles and the 5,237 genes on the basis of similarity in their expression pattern across all 53 tumors (Fig. 4*A* and SI Fig. 8). This analysis yielded several groups of clustered genes, which contained basal CKs (*Krt2–5*) and other markers (*Trim29*, *Trp-63*, and *Idb4*) that have been implicated in basal-like breast cancer (9, 30–32). These markers, which are often expressed in human *BRCA1*-mutated breast cancers (9, 32), were also up-regulated in most, if not all, mouse $Brca1^{\Delta/\Delta}$;$p53^{\Delta/\Delta}$ tumors. Increased expression of p63 and CK5 in $Brca1^{\Delta/\Delta}$;$p53^{\Delta/\Delta}$ tumors, compared with $p53^{\Delta/\Delta}$ tumors, could be confirmed by immunohistochemistry (Fig. 4 *B–G*).

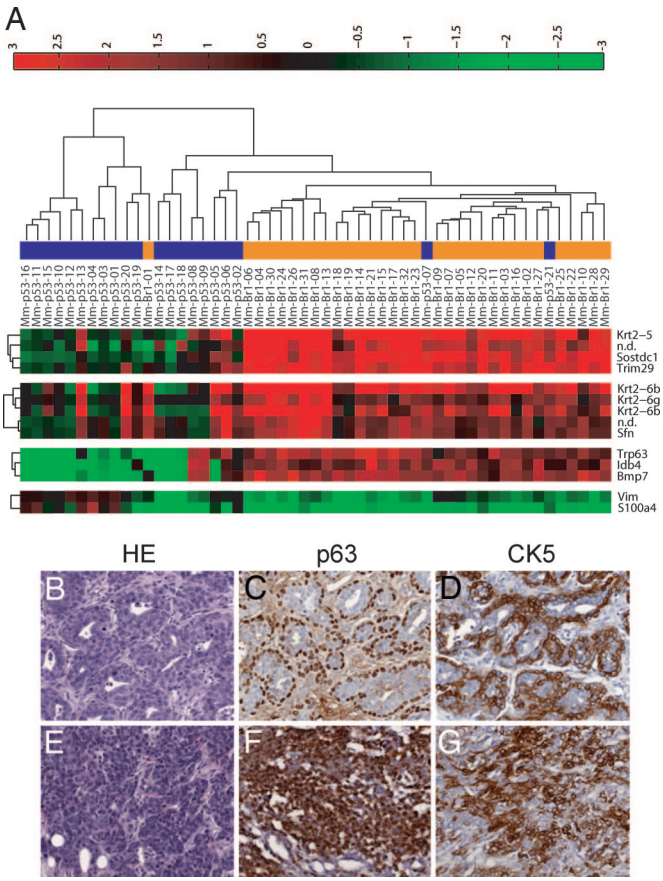

Fig. 4. Mammary tumors from K14*cre*;*Brca1*$^{F/F}$;*p53*$^{F/F}$ female mice display characteristics of basal-like breast cancers. (*A*) Unsupervised hierarchical clustering of gene expression profiles from mammary tumors of K14*cre*;*Brca1*$^{F/F}$;*p53*$^{F/F}$ ($n = 32$) and K14*cre*;*p53*$^{F/F}$ ($n = 21$) mice. Two-dimensional clustering based on Pearson correlation coefficients revealed three branches of genes that contained several markers for basal cell types. The complete heat map of all 5,237 significant genes is depicted in SI Fig. 8. The dendrogram shows that the majority of the *p53*$^{\Delta/\Delta}$ tumors (in blue) were separated from the *Brca1*$^{\Delta/\Delta}$;*p53*$^{\Delta/\Delta}$ tumors (in orange). (*B–G*) Histochemical staining of mammary tumor sections from K14*cre*;*Brca1*$^{F/F}$;*p53*$^{F/F}$ mice (*B–D*) and K14*cre*;*p53*$^{F/F}$ animals (*E–G*), with H&E (*B* and *E*) or with antibodies against p63 (*C* and *F*) and CK5 (*D* and *G*).

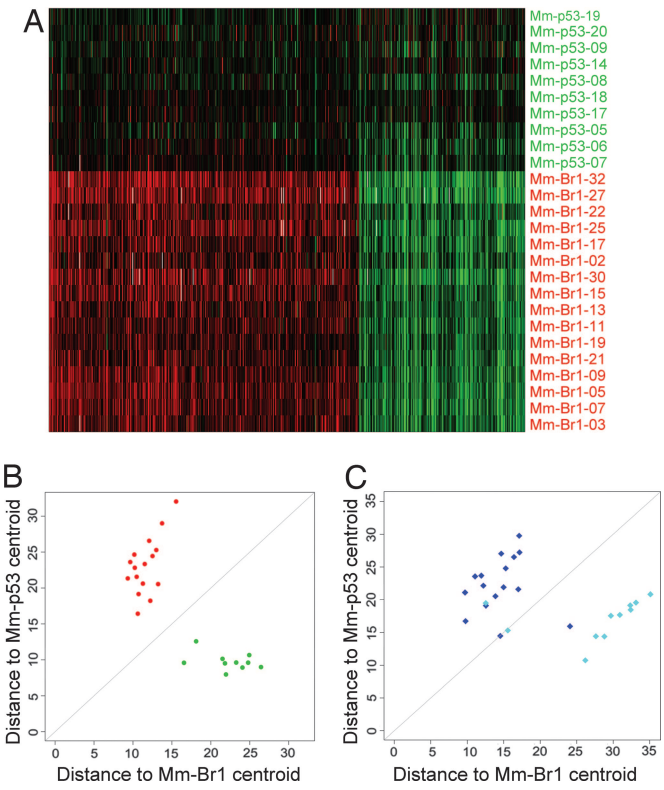

Fig. 5. Supervised classification of mouse mammary tumors. (*A*) Expression data matrix of 646 BRCA1 reporter genes from a training set containing 16 *Brca1*$^{\Delta/\Delta}$;*p53*$^{\Delta/\Delta}$ carcinomas (red) and 10 *p53*$^{\Delta/\Delta}$ carcinomas (green). Each row represents a tumor, and each column represents a gene. (*B*) Supervised classification of individual tumors from the training set according to their Euclidean distances to the centroids of mouse *Brca1*$^{\Delta/\Delta}$;*p53*$^{\Delta/\Delta}$ mammary tumors and *p53*$^{\Delta/\Delta}$ tumors, respectively. (*C*) Supervised classification of an independent validation series containing 16 *Brca1*$^{\Delta/\Delta}$;*p53*$^{\Delta/\Delta}$ tumors (dark blue diamonds) and 11 *p53*$^{\Delta/\Delta}$ tumors (light blue diamonds). Most mammary tumors in the validation series (23/27) were correctly classified by the 646 reporter genes.

Supervised Classification of Mouse Mammary Tumors. To identify a group of reporter genes that could distinguish mouse *Brca1*$^{\Delta/\Delta}$;*p53*$^{\Delta/\Delta}$ tumors from *p53*$^{\Delta/\Delta}$ tumors, we performed supervised classification based on significance analysis of microarrays with a training set of 16 *Brca1*$^{\Delta/\Delta}$;*p53*$^{\Delta/\Delta}$ carcinomas and 10 *p53*$^{\Delta/\Delta}$ carcinomas. We obtained a set of 646 genes (false discovery rate = 0.012) for which expression was either decreased or increased in the *Brca1*$^{\Delta/\Delta}$;*p53*$^{\Delta/\Delta}$ tumors, compared with the *p53*$^{\Delta/\Delta}$ tumors (Fig. 5*A* and SI Table 4). A nearest centroid classifier based on the 646 BRCA1 reporter genes was capable of classifying the *Brca1*$^{\Delta/\Delta}$;*p53*$^{\Delta/\Delta}$ and *p53*$^{\Delta/\Delta}$ tumors from the training set with 100% accuracy (Fig. 5*B*). Moreover, an 85% (23 of 27) correct classification rate was obtained with the *Brca1* classifier for a validation series of 16 *Brca1*$^{\Delta/\Delta}$;*p53*$^{\Delta/\Delta}$ and 11 *p53*$^{\Delta/\Delta}$ tumors that were not part of the training data set (Fig. 5*C*). Gene ontology (GO) analysis showed significant overrepresentation of the 646 optimal BRCA1 reporter genes in a number of biological processes, including cell differentiation, cell cycle, and chromatin modification (SI Table 5 and SI Fig. 9).

Cross-Species Comparison by Unsupervised Clustering. To determine whether the molecular signatures of mouse *Brca1*$^{\Delta/\Delta}$;*p53*$^{\Delta/\Delta}$ mammary tumors resembled those of human *BRCA1*-mutated breast cancers, we examined the relationships among a group of 53 mouse mammary tumors (21 *p53*$^{\Delta/\Delta}$ tumors and 32 *Brca1*$^{\Delta/\Delta}$;*p53*$^{\Delta/\Delta}$ tumors) and 44 human breast tumors (16 ER-negative *BRCA1* tumors and 28 ER-negative sporadic tumors) using unsupervised clustering (Fig. 6*A* and SI Fig. 10). The first bifurcation of the hierarchical clustering dendrogram identifies two clusters of tumors, which represent nonrandom samplings from the complete population (χ^2 test; $P = 3.7 \times 10^{-4}$ and $P = 2.5 \times 10^{-5}$, respectively). Mouse *p53*$^{\Delta/\Delta}$ tumors are overrepresented in Cluster 1 (hypergeometric test; $P = 6.9 \times 10^{-7}$), and mouse *Brca1*$^{\Delta/\Delta}$;*p53*$^{\Delta/\Delta}$ tumors are overrepresented in Cluster 2 (hypergeometric test; $P = 4.2 \times 10^{-11}$). The human sporadic ER-negative tumors show a significant association with Cluster 1, whereas the human *BRCA1* tumors show a significant association with Cluster 2 (χ^2 test; $P = 0.035$). Hence, human ER-negative sporadic breast cancers cluster together with mouse *p53*$^{\Delta/\Delta}$ mammary tumors, whereas human *BRCA1* tumors cocluster with mouse *Brca1*$^{\Delta/\Delta}$;*p53*$^{\Delta/\Delta}$ tumors.

Cross-Species Comparison by Gene Set Enrichment Analysis (GSEA). To further explore the similarity between the mouse and human tumors, we used GSEA (33). Based on the expression of 7,127 nonredundant, annotated genes represented on both mouse and human microarray platforms, GSEA was applied to test association between expression of the genes in a gene set and the class labels (i.e., *Brca1*$^{\Delta/\Delta}$;*p53*$^{\Delta/\Delta}$ vs. *p53*$^{\Delta/\Delta}$ for mouse tumors, and *BRCA1*-mutated vs. sporadic ER-negative for human tumors).

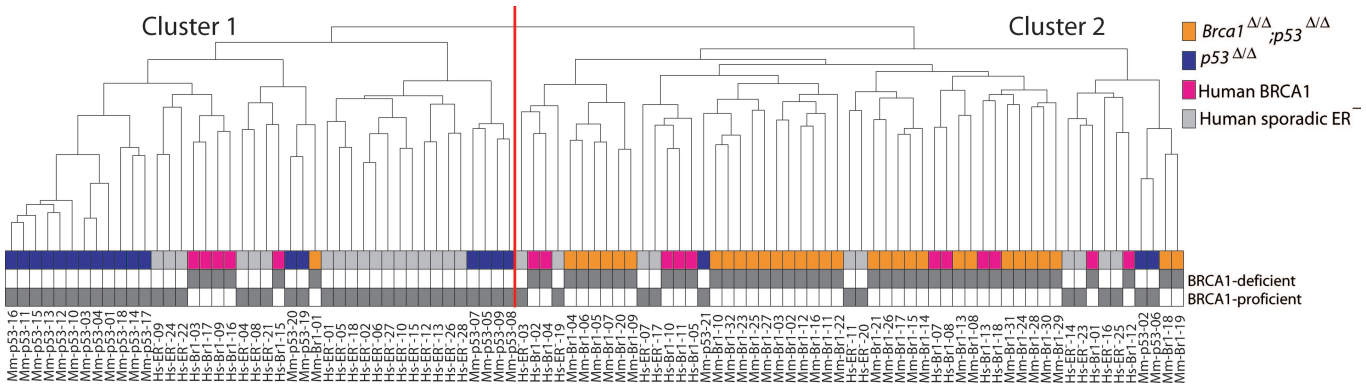

Fig. 6. Cross-species comparison of mouse and human BRCA1-deficient breast cancers. Unsupervised hierarchical clustering was used to compare gene expression profiles of human breast cancer samples from 16 *BRCA1* mutation carriers (pink) and 28 sporadic ER-negative cases (gray), with profiles of 32 mammary tumors from K14*cre*;*Brca1*$^{F/F}$;*p53*$^{F/F}$ female mice (orange) and 21 tumors from K14*cre*;*p53*$^{F/F}$ female mice (blue). Most mouse *Brca1*$^{\Delta/\Delta}$;*p53*$^{\Delta/\Delta}$ and human *BRCA1*-mutated tumors (42 of 48) are interspersed and cluster together in a single branch of the dendrogram. The complete heat map of all 5,410 significant genes is shown in SI Fig. 10.

SI Fig. 11 *B* and *C* depicts scatter plots of the mouse and human maximum enrichment scores for 980 gene sets of the GO hierarchy (www.geneontology.org) and 424 gene sets of the MSigDb C2 pathways database (www.broad.mit.edu/gsea), respectively. Overall, similar sets of genes exhibit equal levels of association between the gene expression and the class labels for both species, meaning that if a given gene set is predictive for the class label of the human tumors, the same set is also likely to be predictive for the class label of the mouse tumors. In support of this, a significant overlap (24/98) is observed for the top-10% GO gene sets with maximal enrichment scores based on human data and mouse data, respectively (hypergeometric test; $P = 7.7 \times 10^{-6}$). The overlap of the top 10% of the MSigDb gene sets (11 of 42) also is significant ($P = 1.1 \times 10^{-3}$). Several of these overlapping top 10% of the gene sets are associated with processes in which BRCA1 is implicated, such as recombinatorial repair, mitotic recombination, telomere maintenance, X-inactivation, and transcriptional regulation (SI Table 6).

Discussion

To create a mouse model for BRCA1-associated breast cancer, we have exploited two main characteristics of *BRCA1*-mutated tumors: the frequent occurrence of *TP53* mutations and the basal-like phenotype characterized by the expression of basal epithelial markers such as CK5 and CK14. Using Cre-loxP technology, we targeted somatic mutation of both *Brca1* and *p53* specifically to CK14-expressing (mammary) epithelial cells. The resulting K14*cre*;*Brca1*$^{F/F}$;*p53*$^{F/F}$ mouse model shows effective cooperation of BRCA1 and p53 in mammary tumorigenesis and a lack of haploinsufficiency for BRCA1 in mammary tumor suppression. The majority of *Brca1*$^{\Delta/\Delta}$;*p53*$^{\Delta/\Delta}$ mammary tumors are solid carcinomas that resemble high-grade IDC-nos in humans.

Our histopathological and molecular analyses showed that *Brca1*$^{\Delta/\Delta}$;*p53*$^{\Delta/\Delta}$ mammary tumors recapitulate several features of both human *BRCA1*-mutated hereditary breast cancers and sporadic basal-like breast cancers. Most *Brca1*$^{\Delta/\Delta}$;*p53*$^{\Delta/\Delta}$ tumors are highly proliferative, ER-negative carcinomas with a high degree of genomic instability, pushing borders, and expression of basal epithelial markers. The basal-like tumor phenotype might, in part, be explained by the fact that Cre expression in our K14*cre* transgenic mice is driven by the basal CK14 gene promoter, which is active in mammary stem cells (34, 35).

The availability of mammary tumors from both K14*cre*;*p53*$^{F/F}$ and K14*cre*;*Brca1*$^{F/F}$;*p53*$^{F/F}$ mice allowed us to study the role of BRCA1 loss of function in breast oncogenesis via comparative analysis of matched series of BRCA1-proficient and BRCA1-deficient tumors. Gene expression profiling of *Brca1*$^{\Delta/\Delta}$;*p53*$^{\Delta/\Delta}$ mammary tumors and *p53*$^{\Delta/\Delta}$ control tumors showed that BRCA1 loss leads to a more undifferentiated tumor phenotype with increased expression of basal epithelial markers, suggesting that BRCA1 might be causally related to the basal-like tumor phenotype. In support of this, BRCA1 has recently been reported to be required for differentiation of mammary epithelial cells (36).

Further support for our mice as a model for human *BRCA1*-mutated breast cancer came from our cross-species comparisons of microarray expression data from mouse and human breast tumors. Unsupervised clustering of gene expression patterns showed that *Brca1*$^{\Delta/\Delta}$;*p53*$^{\Delta/\Delta}$ mouse mammary tumors are most similar to human *BRCA1* tumors, whereas *p53*$^{\Delta/\Delta}$ mouse tumors are more similar to human sporadic basal-like breast cancers. Similarity between mouse and human BRCA1-deficient tumors is underscored by the fact that *Brca1*$^{\Delta/\Delta}$;*p53*$^{\Delta/\Delta}$ mouse mammary tumors mix with human *BRCA1*-mutated tumors, instead of falling into two separate branches in the dendrogram.

Conventional methods for microarray expression data analysis, such as unsupervised clustering or supervised classification, fail to detect biological processes that are distributed across a gene network and subtle at the level of individual genes. We have therefore used a second analysis method, GSEA, to search for shared relationships between mouse and human *BRCA1* tumors with regard to expression patterns of sets of genes with the same biological function or ontology. GSEA of mouse and human *BRCA1* tumors showed that, overall, functional gene sets exhibit similar levels of correlation between gene expression and the class labels (i.e., BRCA1-proficient vs. BRCA1-deficient) in both species. Hence, gene sets that are predictive for the class label of the human sample are also likely to be predictive for the class label of the mouse sample. Of note, several of the most predictive gene sets are associated with processes in which BRCA1 is implicated, such as recombinatorial repair and mitotic recombination (5), telomere maintenance (37), X-inactivation (38), and transcriptional regulation (39).

In summary, we have generated a K14*cre*;*Brca1*$^{F/F}$;*p53*$^{F/F}$ mouse model that develops BRCA1-deficient mammary tumors that closely mimic human *BRCA1*-mutated breast cancers with basal-like phenotypes. This model may be helpful in predicting responses of human BRCA1-deficient tumors to conventional chemotherapeutics (40), as well as targeted therapeutics such as poly(ADP-ribose) polymerase 1 inhibitors that target cancers with defective homologous recombination repair (41, 42).

Materials and Methods

Mutant Mouse Strains. Generation of conditional *Brca1*^{F} mouse mutants is described in *SI Materials and Methods*. Generation of

conditional $p53^{F}$ mutants and K14*cre* transgenic mice has been described previously (25). All animal experiments were approved by the local ethical review committee.

Southern Blot Analysis and Genotyping. Isolation of high-molecular weight DNA and Southern blot analysis was carried out as described previously (25). Genotyping of the K14*cre* and $p53^{F}$ alleles was performed as described (25). Genotyping of $Brca1^{F}$ and $Brca1^{\Delta}$ alleles are described in *SI Materials and Methods*.

Histology and Immunohistochemistry. Histological and immunohistochemical stainings of tissue sections were performed as described before (43). Primary and secondary antibodies used are listed in *SI Materials and Methods*.

Array-CGH Analysis. Array-CGH analysis of mouse mammary tumors was performed by fluorochrome-reversed pairs of two-color hybridizations of 3K mouse BAC microarrays with fluorescently labeled tumor DNA and normal (spleen) DNA from the same animals as described (44). The Rosetta error model was used to calculate weighted averages and statistical confidence levels (29, 44). All values with P values <0.01 were considered to represent significant CNAs. To quantify the difference in genomic instability between $p53^{\Delta/\Delta}$ and $Brca1^{\Delta/\Delta};p53^{\Delta/\Delta}$ tumors, the total number of significant BACs was summed for all tumors in each tumor group, and a two-sided t test was used to determine statistical significance of the observed differences in values calculated for both groups.

Gene Expression Profiling. Methods for RNA extraction, RNA amplification, microarray hybridization, and data processing are described in *SI Materials and Methods*. For unsupervised clustering and supervised classification, the number of gene features was reduced from 18,173 to 5,237 by excluding genes with >10% missing value, as well as genes that showed significant changes in expression ($\log_2$ ratio > 1 or < -1) in <10% of the samples.

Unsupervised Clustering and Supervised Classification. 2D unsupervised hierarchical clustering was performed using the Pearson correlation as a distance measure and complete linkage. Significance analysis of microarrays analysis (www.bioconductor.org/packages/1.8/bioc/html/siggenes.html) (45) was used to identify a group of mouse BRCA1 reporter genes, which could separate mouse $Brca1^{\Delta/\Delta};p53^{\Delta/\Delta}$ tumors from $p53^{\Delta/\Delta}$ tumors in the training set. Supervised classification was performed by calculating the Euclidean distance of each tumor to the centroid of the mouse $Brca1^{\Delta/\Delta};p53^{\Delta/\Delta}$ tumors and $p53^{\Delta/\Delta}$ tumors, respectively. Tumors used for training and validations are indicated in SI Tables 2 and 3.

GO Analysis of Mouse BRCA1 Reporter Genes. GO analysis of mouse BRCA1 reporter genes was performed using the Gene Set Analysis Toolkit (www.bioinfo.vanderbilt.edu/webgestalt).

Cross-Species Comparison of Microarray Data. Methods used for unsupervised hierarchical clustering and GSEA analysis of microarray expression data from human and mouse tumors are described in *SI Materials and Methods*.

We thank K. van Veen-Buurman and K. van 't Wout (Netherlands Cancer Institute) for blastocyst injections; Kreatech Biotechnology for providing ULS reagents; M. Mandjes-van Uitert for statistical analysis; the Netherlands Cancer Institute microarray facility, animal facility, and pathology laboratory for providing excellent service; and R. van Amerongen, K. de Visser, and B. Evers for critically reading the manuscript. This work was supported by Netherlands Organization for Scientific Research Grant ZonMw 917.036.347 (to J.J.), Dutch Cancer Society Grant NKI 2002–2635 (to J.J. and A.B.), and Susan G. Komen Breast Cancer Foundation Grant BCTR 0403230 (to J.J.).

1. Thompson D, Easton DF (2002) *J Natl Cancer Inst* 94:1358–1365.
2. Wooster R, Weber BL (2003) *N Engl J Med* 348:2339–2347.
3. Scully R, Livingston DM (2000) *Nature* 408:429–432.
4. Narod SA, Foulkes WD (2004) *Nat Rev Cancer* 4:665–676.
5. Venkitaraman AR (2002) *Cell* 108:171–182.
6. Lakhani SR, Jacquemier J, Sloane JP, Gusterson BA, Anderson TJ, van de Vijver MJ, Farid LM, Venter D, Antoniou A, Storfer-Isser A, *et al.* (1998) *J Natl Cancer Inst* 90:1138–1145.
7. Lakhani SR, Reis-Filho JS, Fulford L, Penault-Llorca F, van de Vijver MJ, Parry S, Bishop T, Benitez J, Rivas C, Bignon YJ, *et al.* (2005) *Clin Cancer Res* 11:5175–5180.
8. Perou CM, Sorlie T, Eisen MB, van de Rijn M, Jeffrey SS, Rees CA, Pollack JR, Ross DT, Johnsen H, Akslen LA, *et al.* (2000) *Nature* 406:747–752.
9. Sorlie T, Tibshirani R, Parker J, Hastie T, Marron JS, Nobel A, Deng S, Johnsen H, Pesich R, Geisler S, *et al.* (2003) *Proc Natl Acad Sci USA* 100:8418–8423.
10. Turner N, Tutt A, Ashworth A (2004) *Nat Rev Cancer* 4:814–819.
11. Evers B, Jonkers J (2006) *Oncogene* 25:5885–5897.
12. Ludwig T, Chapman DL, Papaioannou VE, Efstratiadis A (1997) *Genes Dev* 11:1226–1241.
13. Hakem R, de la Pompa JL, Sirard C, Mo R, Woo M, Hakem A, Wakeham A, Potter J, Reitmair A, Billia F, *et al.* (1996) *Cell* 85:1009–1023.
14. Gowen LC, Johnson BL, Latour AM, Sulik KK, Koller BH (1996) *Nat Genet* 12:191–194.
15. Ludwig T, Fisher P, Ganesan S, Efstratiadis A (2001) *Genes Dev* 15:1188–1193.
16. Xu X, Qiao W, Linke SP, Cao L, Li WM, Furth PA, Harris CC, Deng CX (2001) *Nat Genet* 28:266–271.
17. Brodie SG, Xu X, Qiao W, Li WM, Cao L, Deng CX (2001) *Oncogene* 20:7514–7523.
18. Xu X, Wagner KU, Larson D, Weaver Z, Li C, Ried T, Hennighausen L, Wynshaw-Boris A, Deng CX (1999) *Nat Genet* 22:37–43.
19. Mixon M, Kittrell F, Medina D (2000) *Oncogene* 19:5237–5243.
20. Crook T, Crossland S, Crompton MR, Osin P, Gusterson BA (1997) *Lancet* 350:638–639.
21. Donehower LA, Harvey M, Slagle BL, McArthur MJ, Montgomery CA, Butel JS, Bradley A (1992) *Nature* 356:215–221.
22. Jacks T, Remington L, Williams BO, Schmitt EM, Halachmi S, Bronson RT, Weinberg RA (1994) *Curr Biol* 4:1–7.
23. Purdie CA, Harrison DJ, Peter A, Dobbie L, White S, Howie SE, Salter DM, Bird CC, Wyllie AH, Hooper ML, *et al.* (1994) *Oncogene* 9:603–609.
24. Jonkers J, Berns A (2002) *Nat Rev Cancer* 2:251–265.
25. Jonkers J, Meuwissen R, van der Gulden H, Peterse H, van der Valk M, Berns A (2001) *Nat Genet* 29:418–425.
26. Pihan G, Doxsey SJ (2003) *Cancer Cell* 4:89–94.
27. Fukasawa K, Choi T, Kuriyama R, Rulong S, Vande Woude GF (1996) *Science* 271:1744–1747.
28. Xu X, Weaver Z, Linke SP, Li C, Gotay J, Wang XW, Harris CC, Ried T, Deng CX (1999) *Mol Cell* 3:389–395.
29. Weng L, Dai H, Zhan Y, He Y, Stepaniants SB, Bassett DE (2006) *Bioinformatics* 22:1111–1121.
30. Turner NC, Reis-Filho JS, Russell AM, Springall RJ, Ryder K, Steele D, Savage K, Gillett CE, Schmitt FC, Ashworth A, *et al.* (2007) *Oncogene* 26:2126–2132.
31. Ribeiro-Silva A, Ramalho LN, Garcia SB, Brandao DF, Chahud F, Zucoloto S (2005) *Histopathology* 47:458–466.
32. Foulkes WD, Stefansson IM, Chappuis PO, Begin LR, Goffin JR, Wong N, Trudel M, Akslen LA (2003) *J Natl Cancer Inst* 95:1482–1485.
33. Subramanian A, Tamayo P, Mootha VK, Mukherjee S, Ebert BL, Gillette MA, Paulovich A, Pomeroy SL, Golub TR, Lander ES, *et al.* (2005) *Proc Natl Acad Sci USA* 102:15545–15550.
34. Shackleton M, Vaillant F, Simpson KJ, Stingl J, Smyth GK, Asselin-Labat ML, Wu L, Lindeman GJ, Visvader JE (2006) *Nature* 439:84–88.
35. Stingl J, Eirew P, Ricketson I, Shackleton M, Vaillant F, Choi D, Li HI, Eaves CJ (2006) *Nature* 439:993–997.
36. Furuta S, Jiang X, Gu B, Cheng E, Chen PL, Lee WH (2005) *Proc Natl Acad Sci USA* 102:9176–9181.
37. McPherson JP, Hande MP, Poonepalli A, Lemmers B, Zablocki E, Migon E, Shehabeldin A, Porras A, Karaskova J, Vukovic B, *et al.* (2006) *Hum Mol Genet* 15:831–838.
38. Ganesan S, Silver DP, Greenberg RA, Avni D, Drapkin R, Miron A, Mok SC, Randrianarison V, Brodie S, Salstrom J, *et al.* (2002) *Cell* 111:393–405.
39. Welcsh PL, Lee MK, Gonzalez-Hernandez RM, Black DJ, Mahadevappa M, Swisher EM, Warrington JA, King MC (2002) *Proc Natl Acad Sci USA* 99:7560–7565.
40. Rottenberg S, Nygren AOH, Pajic M, van Leeuwen FWB, van der Heijden I, van de Wetering K, Liu X, de Visser KE, Gilhuijs KG, van Tellingen O, *et al.* (2007) *Proc Natl Acad Sci USA* 104:12117–12122.
41. Farmer H, McCabe N, Lord CJ, Tutt AN, Johnson DA, Richardson TB, Santarosa M, Dillon KJ, Hickson I, Knights C, *et al.* (2005) *Nature* 434:917–921.
42. Bryant HE, Schultz N, Thomas HD, Parker KM, Flower D, Lopez E, Kyle S, Meuth M, Curtin NJ, Helleday T (2005) *Nature* 434:913–917.
43. Derksen PW, Liu X, Saridin F, van der Gulden H, Zevenhoven J, Evers B, van Beijnum JR, Griffioen AW, Vink J, Krimpenfort P, *et al.* (2006) *Cancer Cell* 10:437–449.
44. Chung YJ, Jonkers J, Kitson H, Fiegler H, Humphray S, Scott C, Hunt S, Yu Y, Nishijima I, Velds A, *et al.* (2004) *Genome Res* 14:188–196.
45. Tusher VG, Tibshirani R, Chu G (2001) *Proc Natl Acad Sci USA* 98:5116–5121.